Asia-Pacific Journal of Science and Technology: Volume: 29. Issue: 06. Article ID.: APST-29-06-01. Research Article

APST

Asia-Pacific Journal of Science and Technology

https://www.tci-thaijo.org/index.php/APST/index

Published by Research Department,
Khon Kaen University, Thailand

Experimental investigation and mathematical modeling of silkworm pupae drying using far-infrared radiation combined with hot air

Thawatchai Supavititpatana[1] and Poomjai Sa-adchom[2,*]

[1]Division of Food Science and Technology, Faculty of Food and Agricultural Technology, Pibulsongkram Rajabhat University, Phitsanulok, Thailand
[2]Department of Mechanical Engineering, Faculty of Engineering, Rajamangala University of Technology Lanna, Tak, Thailand
[*]Corresponding author: poomjai.s@gmail.com

Received 15 October 2023
Revised 15 January 2024
Accepted 31 January 2024

Abstract

This study aimed to investigate the effect of far-infrared radiation (FIR) power and the position of FIR heaters on the drying kinetics, specific energy consumption (SEC), color, and hardness of silkworm pupae undergoing drying using FIR (at 0, 100, 300, and 500 W) combined with forced convection heat transfer using hot air (at 110 °C). The FIR heaters were positioned in two ways: (1) at the top of the drying chamber, and (2) both at the top and bottom of the drying chamber. The silkworm pupae were dried to a final moisture content of less than 5% on a wet basis (w.b.). Eight mathematical models were analyzed to find the best one for describing the drying behavior of silkworm pupae. Based on the experimental results, an increased FIR power led to decreased drying time and SEC, as well as an increase in product temperature and hardness of the dried silkworm pupae. Drying silkworm pupae using higher FIR power resulted in lower lightness but higher redness and yellowness compared to those dried using lower FIR power. The position of FIR heaters did not have a significant impact on the drying time, product temperature, SEC, color, and hardness of the dried silkworm pupae. The results obtained from fitting the experimental data to mathematical drying models showed that the Page model was the best for describing the drying behavior of silkworm pupae. Additionally, the effective moisture diffusivity (D_{eff}) values of silkworm pupae ranged between 1.13×10^{-8} and 1.81×10^{-8} m^2/s.

Keywords: Drying, Far-infrared radiation, Hot air, Mathematical modeling, Silkworm pupae

1. Introduction

Silkworm pupae are the intermediate stage of development between the larval and adult stages of the silkworm moth. They are typically cylindrical in shape and vary in size and color, depending on the species [1]. Silkworm pupae are consumed as food in various cultures. They are rich in protein (about 55.6% on a dry matter basis) [2], essential amino acids, fat, fiber, and minerals such as calcium, iron, and magnesium [3]. Additionally, silkworm pupae have health-promoting properties since they contain bioactive peptides, which exhibit antioxidative, antihypertensive, antimicrobial, and immunomodulatory activities [4]. However, silkworm pupae have a short shelf life and are prone to spoilage. As a result, they are often dried and processed to extend their shelf life, prevent spoilage, and enhance their quality.

Drying silkworm pupae involves removing moisture from the pupae to increase their shelf life and make them suitable for human consumption. The process typically begins by washing the pupae in water to remove impurities, followed by blanching them in boiling water. After blanching, the pupae are drained and dried using one of several methods, including sun-drying, hot air-drying, or microwave-drying. Sun-drying is a traditional method used to dry silkworm pupae by spreading them out in the sun for several hours until they are completely dry. Kathyayini and Manvi (2022) [5] investigated a sun-drying process of silkworm pupae starting from an initial moisture content of 80.1% wet basis (w.b.) and ending with a final moisture content of around 8.5% w.b. They used an

average drying air temperature of 30.85 °C and observed that the drying process required about 23 hours. However, this method is weather-dependent and can result in uneven drying and contamination by insects, dust, and other debris, even though it is low-cost and simple to implement. Another drying method is air drying, which involves using hot air to remove moisture from silkworm pupae. The pupae are placed on a tray and their moisture removed in a dryer at air temperatures ranging from 50 to 80 °C [6, 7] for several hours until the desired moisture content is achieved. Srikaew and Songsermpong [7] found that hot air drying at 60, 70, and 80 °C for 16, 14, and 10 hours, respectively, reduced the water activity of silkworm pupae to less than 0.6, which effectively prevents the growth of molds, yeasts, and bacteria. Additionally, this method is faster than sun-drying and can be better controlled. However, it also requires more equipment and energy. Microwave drying is another method used to dry silkworm pupae. It is gaining popularity due to its energy efficiency and reduced drying times. In this method, the pupae are placed in a microwave oven with a power output of 100 to 700 W [7-9] for several minutes until they are dry. According to Mishyna et al. [9], drying silkworm pupae using a microwave dryer at 700 W in 13 1-minute intervals, with a 1-minute break between these intervals, resulted in a higher protein content, 60.4%, compared to pupae dried using a hot air dryer at 60 °C for 24 hours. However, microwave drying requires careful control of microwave power and exposure time to prevent overheating and product quality deterioration.

There are several methods available for drying silkworm pupae. Each has its advantages and disadvantages. The choice of drying methods depends on factors such as cost, equipment availability, and desired quality of the final product.

Recently, a drying process using a combination of far-infrared radiation (FIR) and forced convection hot air (HA) has gained increasing interest due to its capability to utilize both radiant and convective heat transfer to remove moisture from products. In this process, the drying product is exposed to an FIR source. This directly heats the product's surface and heat is conducted to its interior, causing internal moisture to evaporate [10]. Simultaneously, HA circulates around the product, transferring heat to its surface. This heat is conducted from the surface into the product's interior to further evaporate moisture. This method is effective in reducing both drying time and energy consumption [11], as it simultaneously utilizes two types of heat transfer and results in high-quality dried products [12]. This approach is commonly used in the food industry, where it is important to quickly dry food products without compromising their quality.

Research has been conducted on drying various food products using FIR combined with HA, including bananas [13], chrysanthemums [14], carrots [15], chives [16], and turmeric [17]. However, no research has been done on drying silkworm pupae using a combination of FIR and HA. This study aimed to investigate the effect of FIR power (0, 100, 300, and 500 W) and the position of the FIR heaters ((1) FIR heaters positioned at the top of the drying chamber, and (2) FIR heaters positioned both at the top and bottom of the drying chamber) on the drying kinetics, specific energy consumption, color, and hardness of silkworm pupae undergoing drying. Additionally, the drying kinetics of silkworm pupae were analyzed using eight mathematical models to find an appropriate model that could describe their drying behavior. The results of this study provide valuable insights into potential applications of FIR in the food industry, especially in drying insects for human consumption.

2. Materials and methods

2.1 Sample preparation

Eri silkworm (*Samia cynthia ricini*) pupae, which had been frozen in a cold room at a temperature of -18 °C for 10 days, were purchased from a shop in the Mueang District, Tak Province, Thailand. A group of frozen silkworm pupae, each approximately 2.5 cm long and weighing about 2 g, was selected and stored for 24 hours in a refrigerator set at a temperature of 5 °C. Afterwards, the pupae were blanched in boiling water for 10 minutes to ripen and soften them. This process was carried out to enhance the drying rate, minimize the drying time, and prevent the occurrence of abnormal product odors as well as the enzymatic browning reaction [7]. Finally, the pupae were drained for 10 minutes and stored in a plastic box in preparation for drying.

2.2 Experimental set-up

Figure 1 shows a schematic diagram of the closed-loop dryer used in this study that combined far-infrared radiation lamps and hot air. The dryer was comprised of several components, including a forward-curved blade centrifugal fan (No. 1) powered by a 1-hp electric motor (Toshiba, model IK, Japan), a motor speed controller (Reckon, model RK-2000, Thailand) (No. 2), a 2.5 kW finned heater (No. 3), a PID temperature controller (Toho, model TTM-004-P-A, Japan) (No. 4), a type-K thermocouple (No. 5), a circular mesh tray with a diameter of 30 cm and a number 10 mesh (No. 6) driven by a 25 W electric motor (Oriental, model 4IK25RGN-C, Japan) (No. 7), four FIR heaters, each with an electrical power of 250 W (Infrapara, model AW-2-250, Thailand) (No. 8), a slide voltage regulator (Union, model TDGC2-series, Thailand) (No. 9), a digital clamp meter (Sanwa, model

DCM60L, Japan) (No. 10), an electric power meter (Dai-ichi, model DD28, Thailand) (No. 11), a 3-inch diameter butterfly valve (No. 12), and a 3-inch pipe system (No. 13).

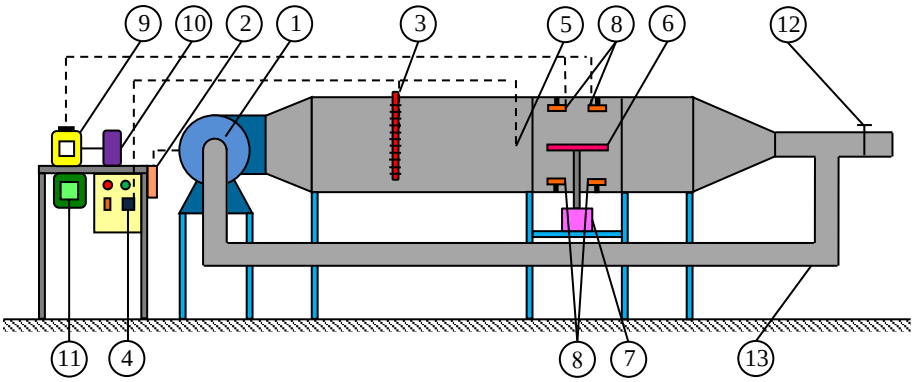

Figure 1 Schematic diagram of a closed-loop dryer that combined far-infrared radiation and hot air, (1) centrifugal fan, (2) motor speed controller, (3) finned heater, (4) PID temperature controller, (5) thermocouple, (6) circular mesh tray, (7) electric motor, (8) FIR heaters, (9) slide voltage regulator, (10) digital clamp meter, (11) electric power meter, (12) butterfly valve, and (13) pipe system.

Operation of the dryer started with air flowing through the finned heater before entering the drying chamber. The hot air temperature was set to 110 °C using a PID temperature controller, while the average airflow rate was controlled at 0.067 kg/s using a motor speed controller. After that, the hot air entered the drying chamber and passed over the surface of the product, which caused moisture to evaporate and be carried away by air. Additionally, FIR heaters were installed on the walls of the drying chamber and positioned 10 cm away from the surface of the drying product. This setup enabled efficient transfer of heat to the product without causing damage or overheating. Two configurations of FIR heaters were tested in the experiments. In the first, two FIR heaters were positioned at the top of the drying chamber, as shown in Figure 2(A). The second configuration used two FIR heaters at the top, and another two FIR heaters at the bottom of the drying chamber, as shown in Figure 2(B). The input voltage was controlled using a slide voltage regulator to adjust the FIR power to 0, 100, 300, and 500 W levels, and the input current was measured using a digital clamp meter. Heat from FIR was conducted into the product, transferring heat to the water molecules within, causing moisture evaporation. Then, the hot air flowed along the loop pipe back to reuse about 80% of the total hot air, while the remaining 20% of the hot air was released into the environment through the butterfly valve to discharge moisture from the dryer [18]. The dryer and air ducts were covered with fiberglass insulation to minimize heat losses to the surroundings.

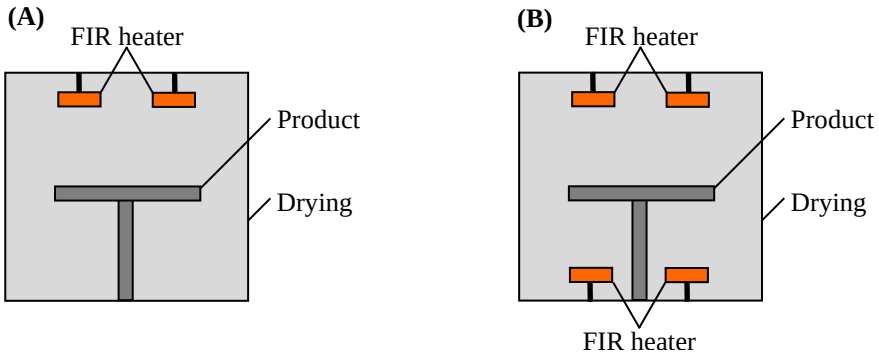

Figure 2 Two positions of the FIR heaters were tested in the experiments, (A) two FIR heaters were positioned at the top of the drying chamber, and (B) two FIR heaters were positioned at the top and another two FIR heaters were positioned at the bottom of the drying chamber.

2.3 Methods

Silkworm pupae, with an initial moisture content of approximately 75% w.b., were weighed to 500 g and placed on a circular tray with a mesh bottom. The tray was rotated at 14.5 rpm to ensure that the silkworm pupae were evenly exposed to heat during the drying process. The experiment utilized FIR in combination with HA convection to dry the silkworm pupae. The experimental conditions included adjusting the FIR power to 0, 100, 300, and 500 W, and setting the HA temperature at 110 °C, with an average airflow of 0.067 kg/s. Two FIR heater

positions were tested in the experiments, as illustrated in Figure 2. The silkworm pupae were dried until the final moisture content was less than 5% w.b. This final moisture content was the same as that of dried silkworm pupae purchased from a local market.

An electronic balance (Sartorius, model CP3202S, Germany) with a precision of ±0.01 g was used to weigh silkworm pupae at 15-min drying intervals (15, 30, 45, 60, ..., 120 minutes) outside of the drying chamber. Moisture content of the silkworm pupae was measured using an AOAC method [19]. The experiments were conducted three times. Results were reported as the mean and standard deviation values.

The temperatures of the silkworm pupae in each experiment were measured using 0.6 mm diameter type-K thermocouples, which were connected to a digital display (Lutron, model TM-947SD, Taiwan). Four thermocouples were inserted into the centers of silkworm pupae, as shown in Figure 3, and the resulting values were used to calculate the average temperature of the silkworm pupae.

Figure 3 Temperature measurements of silkworm pupae.

2.4 Specific energy consumption

The specific energy consumption (SEC) of FIR combined with HA drying refers to the amount of energy required to remove a unit of moisture from a product during the FIR/HA convection drying process. SEC is an important parameter that is used to evaluate the efficiency of drying processes. A lower SEC indicates greater efficiency, as less energy was required to remove the same amount of moisture from the product. The SEC is calculated using the following equation [20]:

$$SEC = \frac{3.6Q}{m_w} \quad (1)$$

where SEC is the specific energy consumption (MJ/kg_{water}), Q is the energy provided during the drying process (kWh), m_w represents the mass of water that is evaporated during drying (kg_{water}), and 3.6 is a factor to convert kWh to MJ.

2.5 Color

Analysis of dried silkworm pupae color was done using a colorimeter (Konica Minolta, model CR-10 Plus, Japan). Color values were determined based on *L** (whiteness/darkness), *a** (redness/greenness), and *b** (yellowness/blueness) parameters. All experiments were performed in triplicate.

2.6 Hardness

The hardness of the dried silkworm pupae was determined using a texture analyzer (Stable Micro Systems, model TA.XT Plus, UK) equipped with a 2 mm diameter cylindrical probe [20]. The maximum force required to penetrate the sample at a test speed of 1 mm/s was defined as the hardness value (N). Each treatment was replicated ten times, and average hardness values were reported.

2.7 Mathematical modeling of drying

The experimental drying data was analyzed in terms of moisture ratio with respect to drying time. The moisture ratio (MR) of the silkworm pupae at any given time was calculated using Eq. (2).

$$MR = \frac{M_t - M_e}{M_0 - M_e} \quad (2)$$

where MR is the moisture ratio (-), M_t is the moisture content at any drying time (d.b.), M_0 is the initial moisture content (d.b.), and M_e is the equilibrium moisture content (d.b.). The M_e value was relatively small compared to the M_t or M_0 values, especially for drying using far-infrared radiation [21]. Therefore, M_e was set to zero in this study, and MR could be expressed as M_t/M_0.

The mathematical drying models listed in Table 1 were used to fit the MR data of silkworm pupae under different drying conditions. The suitability of each model was assessed by calculating the coefficient of determination (R^2), root mean square error (RMSE), and Chi square (χ^2). The values of R^2, RMSE, and χ^2 were calculated using Eq. (3)-(5) [22] as follows:

$$R^2 = 1 - \left[\frac{\sum_{i=1}^{N} (MR_{pre,i} - MR_{exp,i})^2}{\sum_{i=1}^{N} (\overline{MR}_{pre,i} - MR_{exp,i})^2} \right] \quad (3)$$

$$RMSE = \left[\frac{1}{N} \sum_{i=1}^{N} (MR_{exp,i} - MR_{pre,i})^2 \right]^{1/2} \quad (4)$$

$$\chi^2 = \frac{\sum_{i=1}^{N} (MR_{exp,i} - MR_{pre,i})^2}{N - z} \quad (5)$$

where N is the number of observations, z is the number of constants, $MR_{exp,i}$ and $MR_{pre,i}$ are experimental and predicted moisture ratios, respectively. The most suitable mathematical drying model was identified based on the highest average value of R^2, and the lowest average values of RMSE and χ^2.

Table 1 Mathematical drying models.

Model name	Expression of moisture ratio (MR)	Reference
Lewis	$MR = \exp(-kt)$	[6]
Page	$MR = \exp(-kt^n)$	[6]
Henderson and Pabis	$MR = a \exp(-kt)$	[20]
Wang and Singh	$MR = 1 + at + bt^2$	[6]
Logarithmic	$MR = a \exp(-kt) + c$	[6]
Two-term with 4 parameters	$MR = a \exp(-kt) + b \exp(-k_1 t)$	[20]
Weibull distribution	$MR = (a-b) \exp(-(kt)^n)$	[23]
Diffusion approximation	$MR = a \exp(-kt) + (1-a) \exp(-kbt)$	[20]

Note: MR is the moisture ratio (-), t is the drying time (min), and a, b, c, k, k_1, and n are the drying coefficients.

2.8 Effective moisture diffusivity

A diffusion model based on Fick's second law is the mathematical model used to describe the rate of moisture diffusion within a product during the drying process. For a finite circular cylinder geometry undergoing drying, Fick's second law is expressed as [24]:

$$MR = \frac{32}{5.783\pi^2} \exp\left(-\frac{(5.783 + \beta_1^2) D_{eff}\, t}{r^2}\right) \quad (6)$$

Taking the natural logarithm of Eq. (6) results in a straight line equation of the form y = c + ax, as follows:

$$\ln MR = \ln \frac{32}{5.783\pi^2} + \left(-\frac{(5.783 + \beta_1^2) D_{eff}}{r^2}\right) t \quad (7)$$

where $\beta_1 = \frac{\pi r}{2L}$, MR is the moisture ratio (-), D_{eff} is the effective moisture diffusivity (m^2/s), t is the drying time (s), r is the radius of a silkworm pupa (m) and L is the length of a silkworm pupa (m).

The effective moisture diffusivity (D_{eff}) for drying silkworm pupae was calculated using a slope method, which can be expressed as:

$$D_{eff} = - \frac{ar^2}{(5.783 + \beta_1^2)} \quad (8)$$

where D_{eff} is the effective moisture diffusivity (m^2/s), a is the slope of the plot of ln (MR) as a function of time (t) in Eq. (7), and r is the radius of a silkworm pupa (m).

2.9 Statistical analysis

Statistical analysis was performed using SPSS Version 28 software. One-way analysis of variance (ANOVA) was followed by Duncan's multiple range tests to identify significant differences among silkworm pupae samples under different drying conditions. All statistical tests were conducted with a significance level of $P < 0.05$. Non-linear regression analysis was used for parameter estimation in the mathematical drying models, and the fitness of the models was evaluated using SPSS software.

3. Results and discussion

3.1 Drying kinetics of silkworm pupae

3.1.1 Effect of FIR power on drying kinetics

The drying curves of silkworm pupae using FIR at 0, 100, 300, and 500 W, combined with HA forced convection at 110 °C, are shown in Figure 4. It was found that at the same position of FIR heaters, as the FIR power increased, the intensity of the radiation also increased, leading to a higher rate of heat transfer from the surface to the interior of the product. This increased rate of heat transfer resulted in a more rapid drying time, as the moisture content in the product was rapidly evaporated due to the increased temperature. The results of this research were consistent with those of Doymaz [25], who investigated the drying kinetics of sweet potatoes under various FIR power levels. They found that increasing the FIR power, from 104 to 167 W, resulted in an increased drying rate. Similarly, Adak et al. [26] studied the effect of FIR power on the drying kinetics of strawberries and reported that increasing the FIR power, from 100 to 300 W, resulted in more rapid drying.

The temperature changes of silkworm pupae that were dried using far-infrared radiation at 0, 100, 300, and 500 W, combined with hot air forced convection at 110 °C, are shown in Figure 5. It was found that at the same position of the FIR heaters, the product temperature increased with the FIR power. This occurred because FIR transfers energy and generates heat through radiation, directly heating the product. As the FIR power increased, more energy was emitted, leading to a greater increase in product temperature. These findings are consistent with previous research conducted by Nuthong et al. [27], which investigated the effect of FIR power on longan temperature during FIR and HA combined drying. The study found that increasing the FIR power resulted in a greater longan temperature.

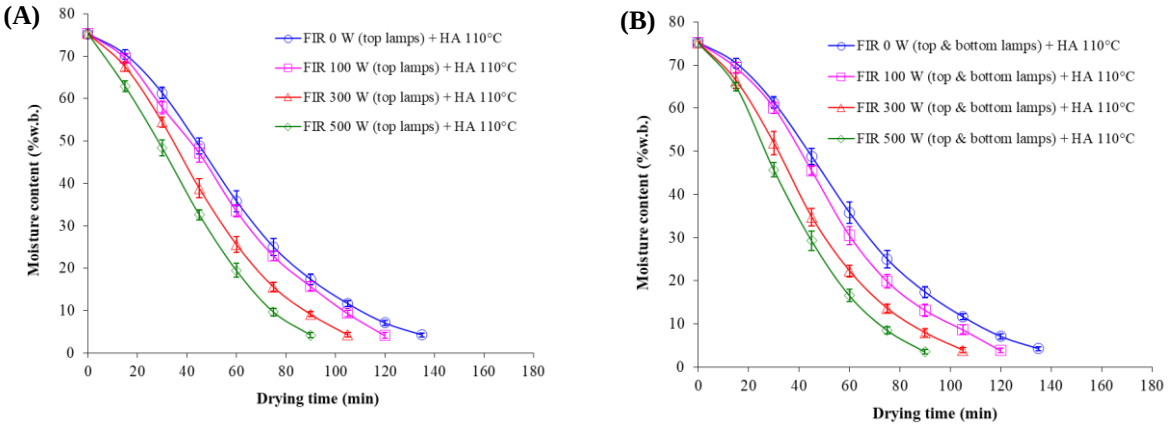

Figure 4 Drying curves of silkworm pupae using far-infrared radiation at 0, 100, 300 and 500 W, in combination with hot air at 110 °C, (A) FIR heaters were positioned only at the top of the drying chamber, and (B) FIR heaters were positioned at both the top and bottom of the drying chamber.

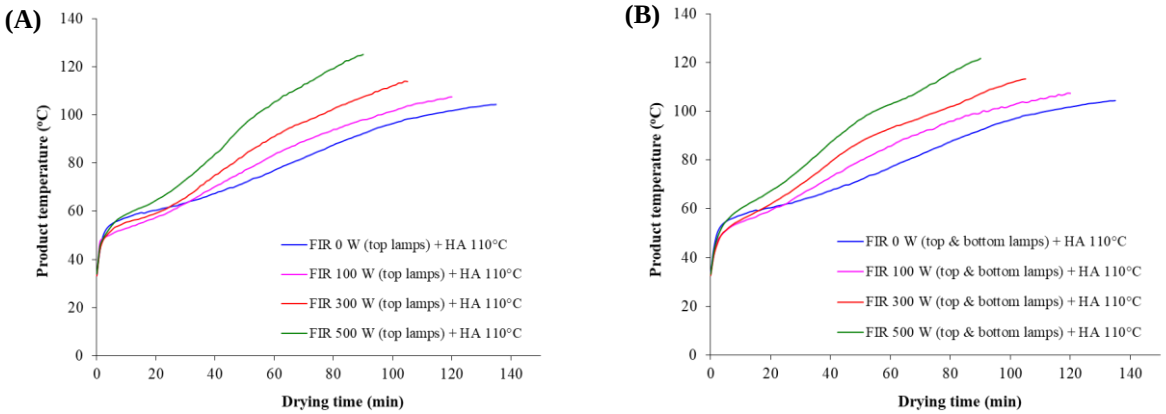

Figure 5 Temperature changes of the silkworm pupa dried using far-infrared radiation at 0, 100, 300 and 500 W, in combination with hot air at 110 °C, (A) FIR heaters were positioned only at the top of the drying chamber, and (B) FIR heaters were positioned both at the top and bottom of the drying chamber.

3.1.2 Effects of the position of FIR heaters on drying kinetics

The drying curves of silkworm pupae, when FIR heaters were positioned only at the top of the drying chamber, and when FIR heaters were positioned both at the top and bottom of the drying chamber combined with hot air forced convection, are shown in Figure 6. At the same FIR power, the position of FIR heaters did not significantly affect the drying curve. This was because the FIR heaters emitted the same power, regardless of their position. It should be noted that two positions of the FIR heaters were tested in the experiment, as illustrated in Figure 2. For example, when two FIR heaters were positioned at the top of the drying chamber (as shown in Figure 2(A)) and set to a power of 500 W, each FIR heater emitted 250 W of power. When two FIR heaters were positioned at the top, and another two FIR heaters were positioned at the bottom of the drying chamber (as shown in Figure 2(B)) set to a power of 500 W, each FIR heater emitted 125 W of power. Therefore, they provided the same energy input to the product being dried. Additionally, position effects of the FIR heaters on drying kinetics has not been previously discussed in the literature.

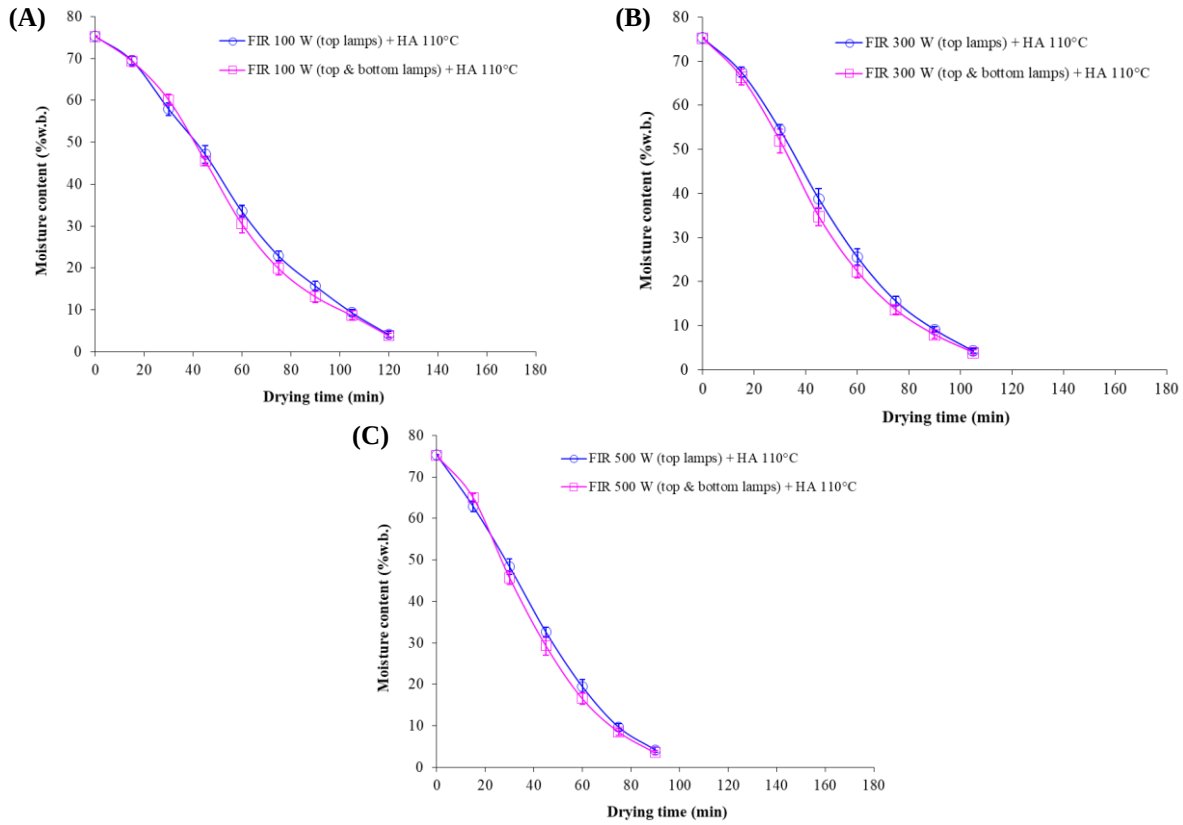

Figure 6 Drying curves of silkworm pupae using a combination of far-infrared radiation and hot air force convection at three different FIR power levels: (A) 100 W, (B) 300 W, and (C) 500 W.

The temperature changes of silkworm pupae when FIR heaters were positioned only at the top of the drying chamber, and when they were positioned both at the top and bottom of the drying chamber undergoing drying of far-infrared radiation combined with hot air convection, are shown in Figure 7. At the same FIR power, the position of FIR heaters did not significantly affect the temperature of the silkworm pupae. This was because FIR heaters emitted a consistent power, resulting in the same amount of energy being applied to the product during the drying process.

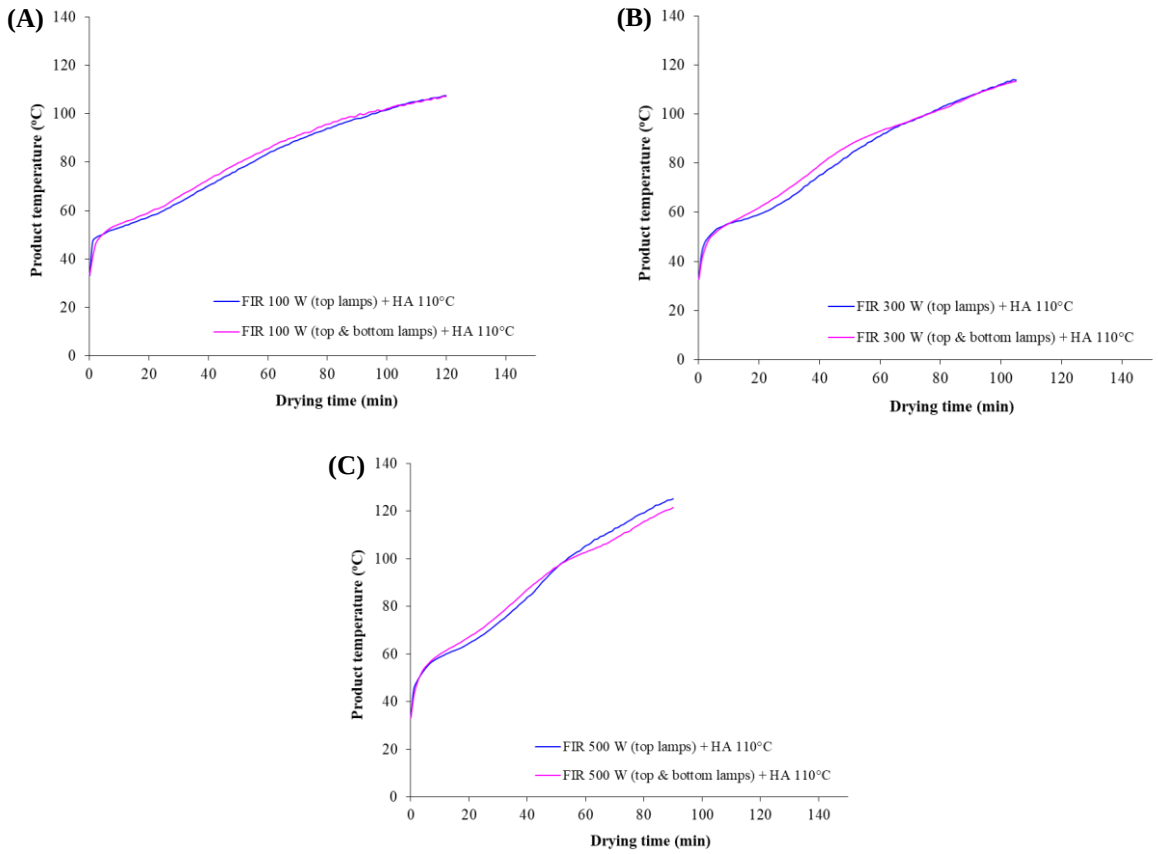

Figure 7 Temperature changes of silkworm pupae that were dried using a combination of far-infrared radiation and hot air convection at three different FIR power levels: (A) 100 W, (B) 300 W, and (C) 500 W.

3.2 *Specific energy consumption of silkworm pupae drying*

3.2.1 Effect of FIR power on specific energy consumption

The SEC values for silkworm pupae drying are shown in Table 2. With the same FIR heater positions, the SEC decreased with increasing FIR power. With lower FIR power, less heat was transferred to the product, resulting in a slower drying rate. As a result, more energy was required to remove the same amount of moisture from the product, leading to an increased SEC. Additionally, at lower FIR power, the temperature difference between the product and the surroundings decreased, which reduced the driving force for heat transfer, resulting in a slower drying rate and higher SEC. The findings of this study are consistent with those of Nosrati et al. [28], who investigated the SEC of rough rice drying in an infrared-assisted vibratory bed dryer. They found that an increase in the FIR intensities from 0 to 2,000 W/m^2 resulted in decreased SEC values.

3.2.2 Effect of the position of FIR heaters on specific energy consumption

In Table 2, it can be seen that at the same FIR power, the position of FIR heaters did not significantly affect the SEC. This was because the amount of energy supplied to the product was constant and did not depend on the position of the heaters. The specific energy consumption is defined as the amount of energy required to remove a unit of moisture from the product. Since the energy input was the same, the specific energy consumption remained constant regardless of the heater position.

Table 2 Specific energy consumption (SEC) of silkworm pupae during drying.

Drying conditions	Position of FIR heaters	Drying time (min)	SEC (MJ/kg_{water})
HA 110 °C	-	135	54.78 ± 1.20^{a}
FIR 100 W + HA 110 °C	At the top of the drying chamber	120	49.70 ± 0.61^{b}
	At the top and bottom of the drying chamber		49.54 ± 1.05^{b}
FIR 300 W + HA 110 °C	At the top of the drying chamber	105	45.80 ± 1.13^{c}
	At the top and bottom of the drying chamber		46.13 ± 1.24^{c}
FIR 500 W + HA 110 °C	At the top of the drying chamber	90	40.66 ± 1.01^{d}
	At the top and bottom of the drying chamber		41.17 ± 0.76^{d}

Values in the same column with different superscripts are significantly different ($P < 0.05$).

3.3 Color of dried silkworm pupae

3.3.1 Effect of FIR power on color of dried silkworm pupae

The color values of dried silkworm pupae are presented in Table 3. It was observed that at the same position of FIR heaters, silkworm pupae dried using two heaters with higher FIR power had significantly lower lightness (L^* value) but higher redness (a^* value) and yellowness (b^* value) than those dried using four heaters at lower individual power settings. Additionally, silkworm pupae dried using hot air at 110°C (HA 110°C) also had significantly lower lightness (L^* value) than those dried using far-infrared radiation at 100, 300, and 500 W combined with hot air convection at 110°C (FIR 100 W + HA 110°C, FIR 300 W + HA 110°C, and FIR 500 W + HA 110°C). Higher FIR powers generated more heat, which caused a greater degree of protein denaturation and Maillard reaction, resulting in darker color with increased redness and yellowness. The findings of this study are consistent with those of Nathakaranakule et al. [29], who investigated the effect of different FIR power levels (0, 250, 350, and 450 W) on the color of dried longan during FIR-assisted drying combined with HA (65°C). Their results showed that as the FIR power increased, the color of the dried longan became darker, with a decreased L^* value (lightness) and an increase in both the a^* value (redness) and b^* value (yellowness).

Table 3 Color of dried silkworm pupae.

Drying conditions	Position of FIR heaters	Drying time (min)	Color values		
			L^*	a^*	b^*
HA 110 °C	-	135	27.63 ± 0.93^{a}	10.92 ± 0.78^{c}	38.71 ± 1.87^{c}
FIR 100 W + HA 110 °C	At the top of the drying chamber	120	24.65 ± 1.16^{b}	12.02 ± 0.76^{c}	40.18 ± 2.27^{c}
	At the top and bottom of the drying chamber		22.90 ± 1.26^{b}	11.23 ± 0.86^{c}	42.01 ± 2.09^{c}
FIR 300 W + HA 110 °C	At the top of the drying chamber	105	19.91 ± 1.20^{c}	13.97 ± 0.62^{b}	46.98 ± 1.82^{b}
	At the top and bottom of the drying chamber		20.89 ± 0.98^{c}	13.40 ± 0.54^{b}	45.80 ± 1.67^{b}
FIR 500 W + HA 110 °C	At the top of the drying chamber	90	16.11 ± 1.03^{d}	15.92 ± 0.70^{a}	50.92 ± 1.75^{a}
	At the top and bottom of the drying chamber		17.80 ± 1.05^{d}	16.96 ± 0.62^{a}	52.67 ± 1.60^{a}
Dried silkworm pupae obtained from a market			26.77 ± 0.89^{a}	8.18 ± 0.66^{d}	30.27 ± 1.72^{d}

Values in the same column with different superscripts are significantly different ($P < 0.05$).

3.3.2 Effect of the position of FIR heaters on color of dried silkworm pupae

In Figure 2, it can be seen that when FIR heaters were positioned only at the top of the drying chamber (shown in Figure 2(A)), the upper side of the pupae was heated centrally. However, in the configuration with FIR heaters positioned both at the top and bottom of the drying chamber (shown in Figure 2(B)), heat was more evenly distributed as both sides of the pupae were heated. However, according to Table 3, it was found that the position of the FIR heaters did not significantly affect the color of the dried silkworm pupae at the same FIR power. This was because the silkworm pupae, whether dried with FIR heaters positioned only at the top of the drying chamber or positioned both at the top and bottom, were exposed to the same amount of heat and radiation. Therefore, the position of the FIR heaters did not significantly impact the temperature of the silkworm pupae, as discussed in

Section 3.1.2. This allows the Maillard reaction to proceed at a similar rate. The Maillard reaction is a complex chemical process that occurs between reducing sugars and amino acids or proteins, leading to browning and flavor development in food. Typically, this reaction takes place during cooking or food processing and is influenced by various factors such as temperature, time, and reactant concentration.

The results in Table 3 also showed that the dried silkworm pupae obtained from a market had significantly lower redness (*a** value) and yellowness (*b** value) than those obtained from this study. This was because these silkworm pupae were dried using hot air at 70 °C for 14 hours, which resulted in a longer drying time compared to those in the current study (90-135 minutes). The longer drying time led to more extensive Maillard reactions, resulting in a darker product color [30].

3.4 Hardness of dried silkworm pupae

3.4.1 Effect of FIR power on hardness of dried silkworm pupae

Hardness values of dried silkworm pupae are presented in Table 4. At the same FIR heater positions, the hardness value of dried silkworm pupae increased with FIR power. This could be attributed to denaturation of proteins in the pupae, which occurs at high temperatures [31], resulting in a harder texture. Additionally, higher FIR power accelerated the rate of moisture reduction in the pupae, which could lead to their increased hardness. This result is consistent with the findings of Song et al. [32], who investigated the effect of FIR power on the quality of dried Chinese Yam chips using a heat pump (50°C) combined with FIR (500, 1,000, and 2,000 W). They observed that increasing FIR power from 500 W to 2,000 W resulted in a significantly increased hardness of dried Chinese Yam chips.

Table 4 Hardness values of dried silkworm pupae.

Drying conditions	Position of FIR heaters	Drying time (min)	Hardness (N)
HA 110 °C	-	135	2.26 ± 0.38^{c}
FIR 100 W + HA 110 °C	At the top of the drying chamber	120	2.35 ± 0.45^{bc}
	At the top and bottom of the drying chamber		2.46 ± 0.57^{bc}
FIR 300 W + HA 110 °C	At the top of the drying chamber	105	2.89 ± 0.46^{ab}
	At the top and bottom of the drying chamber		2.93 ± 0.50^{ab}
FIR 500 W + HA 110 °C	At the top of the drying chamber	90	3.28 ± 0.37^{a}
	At the top and bottom of the drying chamber		3.39 ± 0.39^{a}
Dried silkworm pupae obtained from a market			1.63 ± 0.32^{d}

Values in the same column with different superscripts are significantly different ($P < 0.05$).

3.4.2 Effect of the position of FIR heaters on hardness of dried silkworm pupae

In Table 4, it can be seen that at the same FIR power, the FIR heater position did not significantly affect the hardness of the dried silkworm pupae. Their hardness was mainly determined by their moisture content and the degree of denaturation of their proteins, which were influenced by the drying temperature and time. At the same FIR power, silkworm pupae that underwent drying with FIR heaters positioned only at the top of the drying chamber, and those with FIR heaters positioned both at the top and bottom of the drying chamber, had similar drying times. As a result, they had a similar degree of denaturation and hardness.

The results presented in Table 4 show that the dried silkworm pupae obtained from a market had significantly lower hardness than those obtained from this study. This was because the drying temperature of silkworm pupae in the market was lower than that used in the current study. Drying at a lower temperature resulted in a slower rate of moisture removal from the pupae, which may have caused the protein to denature and lose its structural integrity, resulting in a softer texture. However, drying at a high temperature could have caused rapid moisture removal, leading to the formation of a more rigid and compact structure, resulting in a harder texture [33]. The silkworm pupae in the market were dried using hot air (70°C), whereas the silkworm pupae in this study were dried using FIR (0, 100, 300, and 500 W) combined with hot air convection (110°C).

3.5 Suitable drying conditions for silkworm pupae

In this study, a suitable drying condition for silkworm pupae was achieved using far-infrared radiation at 100 W in combination with hot air convection at 110°C (FIR (100 W) + HA (110°C)). This occurred since silkworm pupae dried using FIR (100 W) + HA (110°C) exhibited higher lightness (*L**) but lower redness (*a** value), yellowness (*b** value), and hardness compared to those dried using FIR (300 W) + HA (110°C) or FIR (500 W) + HA (110°C). Drying with FIR (100 W) + HA (110°C) also resulted in shorter drying times and lower

SEC compared to drying with HA (110°C) alone. However, silkworm pupae dried using FIR (100 W) + HA (110°C) still had significantly higher hardness than the dried silkworm pupae available in the market. Additionally, the hardness of silkworm pupae dried using FIR (100 W) + HA (110°C) was lower than reported by Paengkanya [8], with the hardness of dried silkworm pupae ranging from 3.08±1.35 to 7.60±1.88 N, and Wiset et al. [20], with hardness values ranging from 4.50±0.93 to 7.44±0.85 N.

Based on the experimental results, the position of FIR heaters did not significantly affect the drying curve, temperature of silkworm pupae, SEC, and the color and hardness of the dried silkworm pupae, at the same FIR power. Therefore, positioning two FIR heaters at the top of the drying chamber was selected as the optimal condition. This choice reduced equipment costs for FIR heaters as two heaters were required rather than four.

3.6 Mathematical drying models of silkworm pupae

In Section 3.1, it was noted that the position of FIR heaters did not significantly affect the drying curve at the same FIR power. Therefore, the moisture content data of silkworm pupae, which were dried using FIR heaters placed only at the top of the drying chamber, were converted into MR values. The nine mathematical drying models presented in Table 1 were used to fit curves with MR data and drying times to identify the best mathematical model for describing and predicting the drying behavior of silkworm pupae during a FIR process combined with HA drying. The drying coefficients (a, b, c, k, k_1, and n) obtained from these models, as well as the statistical analysis results (R^2, RMSE, and χ^2 values) obtained using Eqs. (3)-(5), are shown in Table 5. The R^2 values ranged from 0.991883 to 0.999539, the RMSE values ranged from 0.003435 to 0.027352, and the χ^2 values ranged from 0.00001859 to 0.00055786. The Page model yielded the highest R^2 value, 0.999539, as well as the lowest RMSE value, 0.003435, and the lowest χ^2 value, 0.00001859. Therefore, the Page model was shown to be the best mathematical model for representing the drying behavior of silkworm pupae. This finding is consistent with the results reported by Wiset et al. [20], who also found that the Page model was the best model for describing the drying behavior of silkworm pupae undergoing a combined microwave and hot air-drying process.

Correlations between the experimental data and the predictions of the Page model for silkworm pupae drying are shown in Figure 8(A), which present the variation in the moisture ratio with drying time under various drying conditions. The experimental and predicted data of the Page model were highly consistent and nearly identical. Additionally, a plot of the experimental data *vs.* the predicted data of the Page model for different drying conditions is shown in Figure 8(B). The data were clustered along straight lines. This result indicates that the Page model was effective in predicting the drying behavior of silkworm pupae using FIR (at powers of 0, 100, 300, and 500 W) combined with HA (at 110°C).

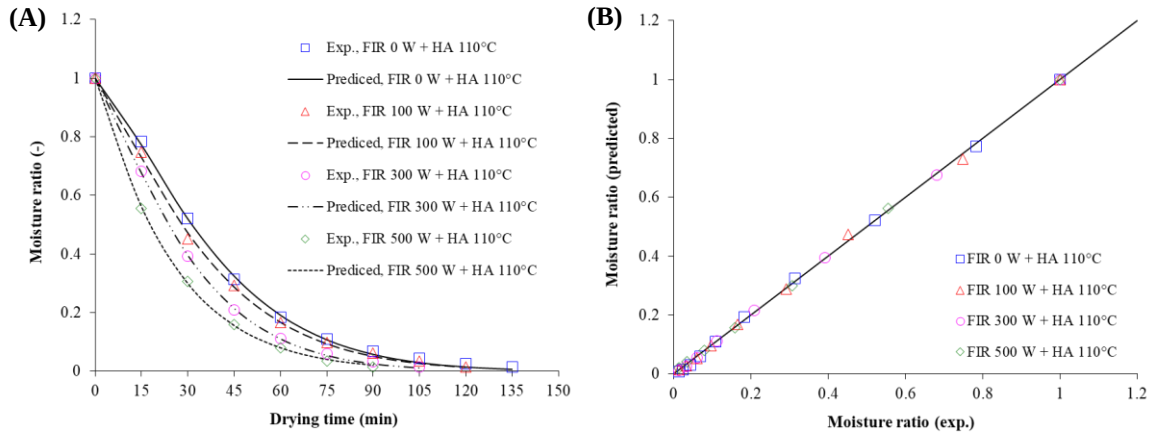

Figure 8 Comparisons between the experimental data and the predictions of the Page model for silkworm pupae drying, (A) variation in moisture ratio with drying time, and (B) plot of experimental results and model predictions.

Table 5 Drying coefficients (a, b, c, k, k_1, and n) obtained from mathematical drying models, and statistical analysis.

Model	FIR (W)	Constants				R^2	RMSE	χ^2
Newton		k						
	0	0.025255				0.989709	0.031264	0.00031171
	100	0.027395				0.993189	0.028405	0.00002095
	300	0.032560				0.994319	0.024301	0.00003460
	500	0.040288				0.999531	0.003791	0.00001271
	Average					0.994187	0.021940	0.00009499
Page		k	n					
	0	0.006936	1.336130			0.999430	0.003593	0.00000016
	100	0.010616	1.251140			0.999102	0.005997	0.00006080
	300	0.013438	1.244690			0.999813	0.002115	0.00000242
	500	0.032435	1.062660			0.999809	0.002033	0.00001096
	Average					0.999539	0.003435	0.00001859
Henderson and Pabis		a	k					
	0	1.052670	0.026428			0.988081	0.023835	0.00025695
	100	1.038910	0.028349			0.992062	0.023067	0.00001087
	300	1.029330	0.033393			0.993523	0.020710	0.00003305
	500	1.005030	0.040466			0.999464	0.003306	0.00001559
	Average					0.993282	0.017729	0.00007912
Wang and Singh		a	b					
	0	-0.017985	0.000081			0.992915	0.011079	0.00001740
	100	-0.019615	0.000097			0.993417	0.006850	0.00031164
	300	-0.022986	0.000133			0.994016	0.000971	0.00023871
	500	-0.027480	0.000189			0.987183	0.027899	0.00029240
	Average					0.991883	0.011700	0.00021504
Logarithmic		a	k	c				
	0	1.099430	0.022736	-0.061318		0.991189	0.019962	0.00010590
	100	1.084370	0.024536	-0.058600		0.994694	0.018790	0.00001131
	300	1.071080	0.029290	-0.052263		0.995760	0.015676	0.00000005
	500	1.023070	0.038043	-0.022473		0.999946	0.000283	0.00000230
	Average					0.995397	0.013678	0.00002989
Two-term with 4 parameters		a	k	b	k_1			
	0	0.612795	0.026428	0.439878	0.026428	0.988081	0.023835	0.00025693
	100	0.597345	0.028349	0.441563	0.028349	0.992062	0.023067	0.00001087
	300	0.584808	0.033393	0.444522	0.033393	0.993523	0.020710	0.00003305
	500	1.738230	0.032419	-0.738605	0.024620	0.999979	0.000692	0.00000179
	Average					0.993411	0.017076	0.00007566
Weibull distribution		a	b	k	n			
	0	549410082	549410081	0.026590	1.191630	0.996287	0.021438	0.00052054
	100	-387658523	-387658524	0.030780	1.069500	0.991248	0.034213	0.00056959
	300	1102014422	1102014421	0.034457	1.128710	0.996774	0.021320	0.00036011
	500	1678017856	1678017855	0.034244	1.223190	0.992988	0.032439	0.00078122
	Average					0.994324	0.027352	0.00055786
Diffusion approximation		a	k	b				
	0	1294.36	0.014380	0.999573		0.992069	0.023267	0.00009063
	100	1376.61	0.016049	0.999621		0.995288	0.020288	0.00001486
	300	1993.36	0.019611	0.999753		0.996508	0.015932	0.00000096
	500	-0.626561	0.024060	1.361620		0.999979	0.000700	0.00000228
	Average					0.995961	0.015047	0.00002718

To calculate the moisture ratio of silkworm pupae at FIR powers of 0, 100, 300, and 500 W using the Page model, the k and n drying coefficients in the model were considered non-linear in terms of the FIR power (E). These non-linear equations, formulated as cubic polynomials, are expressed as:

$$k = x_0 + x_1E + x_2E^2 + x_3E^3 \quad (9)$$

$$n = x_4 + x_5E + x_6E^2 + x_7E^3 \quad (10)$$

where k, and n are the drying coefficients, x_0 to x_7 are constant values, and E is the FIR power (W). The Page model can be expressed as:

$$MR = \exp(-(x_0 + x_1E + x_2E^2 + x_3E^3)t^{(x_4 + x_5E + x_6E^2 + x_7E^3)}) \quad (11)$$

where MR is the moisture ratio (-), and t is the drying time (min). Equation (11) was analyzed using regression analysis to determine the constant values of the equation. The analysis results are presented in Eq. (12), which models the drying behavior of silkworm pupae at FIR powers of 0, 100, 300, and 500 W.

$$MR = \exp(-kt^n) \quad (12)$$

where $k = 0.00693633 + (6.1028\times10^{-5}\times E) - (2.97864\times10^{-7}\times E^2) + (5.55609\times10^{-10}\times E^3)$ and $n = 1.33613 - (0.00141767\times E) + (6.6617\times10^{-6}\times E^2) - (9.8405\times10^{-9}\times E^3)$. The analysis of the Page model in Eq. (12) resulted in an R^2 value of 0.999539, an RMSE of 0.003435, and a χ^2 value of 0.000019. These outcomes indicate that the model is suitable for describing the drying behavior of silkworm pupae.

3.7 Effective moisture diffusivity

The effective moisture diffusivity (D_{eff}) values of silkworm pupae for different drying conditions are presented in Table 6, with values ranging between 1.13×10^{-8} and 1.81×10^{-8} m^2/s. Increasing the power of FIR resulted in increased D_{eff} values. Greater radiation power increased the energy delivered to the product, thereby accelerating the motion of water molecules within it and enhancing heat transfer processes. This resulted in higher moisture diffusion rates within the product. This finding agrees with earlier studies conducted by Ghaboos et al. [34], who found that the D_{eff} value of pumpkin slices increased with FIR power in a combined FIR and vacuum drying process. Additionally, Wiset et al. [20] investigated the D_{eff} values of silkworm pupae undergoing combined microwave (MW) and HA drying. They found that the D_{eff} values of silkworm pupae ranged between 6.6083×10^{-8} and 1.7165×10^{-6} m^2/s, values that are higher than those obtained in the current study. This was because MW drying used electromagnetic radiation to generate heat within the material being dried, leading to more rapid heating and evaporation of moisture. As a result, the D_{eff} values of the product were generally higher in a combination of MW and HA drying compared to our combined FIR and HA drying process.

Table 6 Effective moisture diffusivity of silkworm pupae for each drying method.

Drying conditions	Effective moisture diffusivity (m^2/s)
HA 110 °C	1.13×10^{-8}
FIR 100 W + HA 110 °C	1.36×10^{-8}
FIR 300 W + HA 110 °C	1.59×10^{-8}
FIR 500 W + HA 110 °C	1.81×10^{-8}

4. Conclusion

This study investigated the effects of FIR power and FIR heater position on the drying kinetics, SEC, color, and hardness of dried silkworm pupae. The experiments involved drying using a combination of FIR and HA convection, with FIR power levels of 0, 100, 300, and 500 W, and two positions of FIR heaters: (1) two heaters at the top of the drying chamber, and (2) two heaters at the top and another two heaters at the bottom of the drying chamber. Increased FIR power led to decreased drying times and SEC, as well as an increased product temperature and hardness of the dried silkworm pupae. Silkworm pupae that were dried at higher FIR powers had lower lightness (L^* value) but higher redness (a^* value) and yellowness (b^* value) compared to those dried at lower FIR powers. The position of the FIR heaters did not significantly impact drying time, product temperature, SEC, color (L^*, a^*, and b^* values), or hardness of the dried silkworm pupae. The results obtained from fitting the experimental data to the mathematical drying models showed that the Page model was the best model for describing the drying behavior of silkworm pupae, as it gave a higher R^2 with lower RMSE and χ^2 values. The effective moisture diffusivity (D_{eff}) values of silkworm pupae increased with the FIR power and they ranged between 1.13×10^{-8} and 1.81×10^{-8} m^2/s. Additionally, the study was able to optimize the drying process by identifying the optimal drying conditions, considering the FIR power and the position of FIR heaters, to achieve the desired moisture content and improve the final product quality, while reducing energy consumption and costs.

5. References

[1] Shen G, Wu J, Wang Y, Liu H, Zhang H, Ma S, Peng C, Lin Y, Xia Q. The expression of ecdysteroid UDP-glucosyltransferase enhances cocoon shell ratio by reducing ecdysteroid titre in last-instar larvae of silkworm, *Bombyx mori*. Sci Rep. 2018;8(1):17710.

[2] Hăbeanu M, Gheorghe A, Mihalcea T. Nutritional value of silkworm pupae (*Bombyx mori*) with emphases on fatty acids profile and their potential applications for humans and animals. Insects. 2023;14(3):254.

[3] Akhtar Y, Isman MB. Insects as an alternative protein source. In: Yada RY, editor. Proteins in food processing. 2nd ed. Cambridge: Woodhead Publishing; 2018. p. 263-288.

[4] Altomare AA, Baron G, Aldini G, Carini M, D'Amato A. Silkworm pupae as source of high-value edible proteins and of bioactive peptides. Food Sci Nutr. 2020;8(6):2652-2661.

[5] Kathyayini HS, Manvi D. Experimental investigation of different types of dryers for silkworm pupae drying. Pharma Innovation. 2022;11(3):1033-1038.

[6] Kampagdee M, Poomsa-ad N, Wiset L. Model for drying of Eri silkworm pupae with microwave and hot air combination. JMPEE. 2020;54(2):110-124.

[7] Srikaew C, Songsermpong S. Eri silkworm pupae processing. In: Proceedings of 50th Kasetsart University Annual Conference, Kasetsart University, Bangkok, Thailand, 31 Jan-2 Feb 2012, p. 234-243.

[8] Paengkanya S, Nathakaranakule A, Soponronnarit S. Production of crispy pupae silkworm using drying of microwave combined with hot air. BSJ. 2021;26(3):1476-1489.

[9] Mishyna M, Haber M, Benjamin O, Martinez JJI, Chen J. Drying methods differentially alter volatile profiles of edible locusts and silkworms. J Insects Food Feed. 2020;6(4):405-415.

[10] Riadh MH, Ahmad SAB, Marhaban MH, Soh AC. Infrared heating in food drying: an overview. Dry Technol. 2015;33(3):322-335.

[11] Motevali A, Minaei S, Khoshtaghaza MH, Amirnejat H. Comparison of energy consumption and specific energy requirements of different methods for drying mushroom slices. Energy. 2011;36(11):6433-6441.

[12] Onwude DI, Hashim N, Chen G. Recent advances of novel thermal combined hot air drying of agricultural crops. Trends Food Sci Technol. 2016;57:132-145.

[13] Puangsuwan K, Jumrat S, Muangprathub J, Punvichai T, Karrila S, Pianroj Y. Hybrid infrared with hot air drying of Pisang-Awak banana: kinetics and shrinkage quality. J Food Process Eng. 2021;44(10):13827.

[14] Xu H, Wu M, Wang Y, Wei W, Sun D, Li D, Zheng Z, Gao F. Effect of combined infrared and hot air drying strategies on the quality of chrysanthemum (*Chrysanthemum morifolium* Ramat.) cakes: drying behavior, aroma profiles and phenolic compounds. Foods. 2022;11(15):2240.

[15] Geng Z, Torki M, Kaveh M, Beigi M, Yang X. Characteristics and multi-objective optimization of carrot dehydration in a hybrid infrared /hot air dryer. LWT. 2022;172:114229.

[16] Gu C, Ma H, Tuly JA, Guo L, Zhang X, Liu D, Ouyang N, Luo X, Shan Y. Effects of catalytic infrared drying in combination with hot air drying and freeze drying on the drying characteristics and product quality of chives. LWT. 2022;161:113363.

[17] Jeevarathinam G, Pandiselvam R, Pandiarajan T, Preetha P, Krishnakumar T, Balakrishnan M, Thirupathi V, Ganapathy S, Amirtham D. Design, development, and drying kinetics of infrared-assisted hot air dryer for turmeric slices. J Food Process Eng. 2022;45(6):13876.

[18] Panyayuen A, Lek-ong J, Kunsuwan K, Sa-adchom P. The study of suitable drying time and physical characteristic of pork slices dried using microwave followed by hot air. RMUTP Sci J. 2019;13(1):63-77.

[19] Latimer GW Jr. Official methods of analysis of AOAC international. 22nd ed. Oxford University Press; 2023.

[20] Wiset L, Poomsa-ad N, Duangkhamchan W. Drying characteristics of Eri silkworm snacks as affected by combined microwave and hot air drying. Suranaree J Sci Technol. 2022;29(4):010139.

[21] Sa-adchom P. Drying of tamarind foam-mats using far-infrared radiation combined with a belt conveyor system: Drying kinetics, quality attributes, and mathematical modeling. Eng Appl Sci Res. 2023;50(6):584-596.

[22] Sa-adchom P. Drying kinetics and mathematical modeling of spent coffee grounds drying using the spouted bed technique. Eng Appl Sci Res. 2023;50(4):324-334

[23] Gaikwad PS, Sunil CK, Negi A, Pare A. Effect of microwave assisted hot-air drying temperatures on drying kinetics of dried black gram papad (Indian snack food): Drying characteristics of black gram papad. Appl Food Res. 2022;2(2):100144.

[24] Usub T, Lertsatitthankorn C, Poomsa-ad N, Wiset L, Siriamornpun S, Soponronnarit S. Thin layer solar drying characteristics of silkworm pupae. Food Bioprod Process. 2010;88(2-3):149-160.

[25] Doymaz İ. Infrared drying of sweet potato (*Ipomoea batatas* L.) slices. J Food Sci Technol. 2012;49:760-766.

[26] Adak N, Heybeli N, Ertekin C. Infrared drying of strawberry. Food Chem. 2017;219:109-116.

[27] Nuthong P, Achariyaviriya A, Namsanguan K, Achariyaviriya S. Kinetics and modeling of whole longan with combined infrared and hot air. J Food Eng. 2011;102(3):233-239.

[28] Nosrati M, Zare D, Nassiri SM, Chen G, Jafari A. Experimental and numerical study of intermittent drying of rough rice in a combined FIR-dryer. Dry Technol. 2022;40(10):1967-1979.

[29] Nathakaranakule A, Jaiboon P, Soponronnarit S. Far-infrared radiation assisted drying of longan fruit. J Food Eng. 2010;100(4):662-668.
[30] Sa-adchom P, Swasdisevi T, Nathakaranakule A, Soponronnarit S. Drying kinetics using superheated steam and quality attributes of dried pork slices for different thickness, seasoning and fibers distribution. J Food Eng. 2011;104(1):105-113.
[31] Bischof JC, He X. Thermal stability of proteins. Ann N Y Acad Sci. 2006;1066(1):12-33.
[32] Song X, Hu H, Zhang B. Drying characteristics of Chinese Yam (Dioscorea *opposita Thunb*.) by far-infrared radiation and heat pump. J Saudi Soc Agric Sci. 2018;17(3):290-296.
[33] Voller-Reasonover L, Han I, Acton J, Titus T, Bridges W, Dawson P. High temperature processing effects on the properties of fowl meat gels. Poult Sci. 1997;76(5):774-779.
[34] Ghaboos SHH, Ardabili SMS, Kashaninejad M, Asadi G, Aalami M. Combined infrared-vacuum drying of pumpkin slices. J Food Sci Technol. 2016;53(5):2380-2388.